

Simulation and Experimental Study on Spray Characteristics of Gas-Assisted Urea Spray Gun

Zhifu Zhu*, Peng Chen, Sheng Wang, Jianhua Gui, Wenxiao Wang

College of Physics, Qingdao University, Qingdao, China

Email: *zhuzf686@163.com

How to cite this paper: Zhu, Z.F., Chen, P., Wang, S., Gui, J.H. and Wang, W.X. (2019) Simulation and Experimental Study on Spray Characteristics of Gas-Assisted Urea Spray Gun. *World Journal of Engineering and Technology*, 7, 396-407. <https://doi.org/10.4236/wjet.2019.73029>

Received: May 17, 2019

Accepted: August 3, 2019

Published: August 6, 2019

Copyright © 2019 by author(s) and Scientific Research Publishing Inc. This work is licensed under the Creative Commons Attribution International License (CC BY 4.0).

<http://creativecommons.org/licenses/by/4.0/>



Open Access

Abstract

In this paper, the internal flow field and external spray characteristics of the spray gun were simulated and analyzed by establishing a coupling model of the gas-liquid two-phase flow of the spray gun. The spray particle size and cone angle under different gas path pressures were mainly studied. The calculation results showed that the spray particle size distribution had a large span, but the overall spray particle size was small. The liquid flow and the air pressure had a little influence on the spray cone angle. The spray SMD was tested by a three-dimensional particle dynamic analyzer (PDA), and the spray cone angle was photographed with a high-speed camera. The test data was basically consistent with the simulation results. The experimental results showed that the model can accurately simulate the internal flow field of the spray gun and the atomization process of urea. It can be used to analyze the characteristics of urea spray and provide a theoretical basis for the optimal design of urea spray gun.

Keywords

Urea Spray Gun, Spray Characteristic, SMD, CFD Simulation, Experiment

1. Introduction

With emission regulations increasingly stricter on pollutant emissions, Selective Catalytic Reduction (SCR) has become an important emission reduction technology that meets national V and above emission regulations [1] [2] [3]. SCR technology is also the flue gas denitrification technology that best meets China's national conditions and meets future emission regulations. SCR technology usually sprays 32.5% urea aqueous solution into the exhaust pipe, and then the urea is evaporated, pyrolyzed and hydrolyzed to NH_3 . The nitrogen oxides in the exhaust gas react with NH_3 on the catalyst surface to N_2 and CO_2 to reduce the pollution.

The urea injection system can be divided into a gas-assisted and a non-gas-assisted type, the difference being whether the urea injection system has air-assisted. The gas-assisted urea injection system combined with a suitable nozzle can obtain a smaller and more uniform urea spray. The smaller the SMD (Sauter mean diameter), the better the urea decomposition, thereby improving the reaction efficiency of the SCR system and effectively reduce the risks of urea crystallization.

Numerical simulation is an effective method to shorten the development cycle and save development cost. A large number of scholars have carried out modeling analysis and experimental research on the mixing uniformity of SCR, pyrolysis hydrolysis of urea, catalyst performance and flow field distribution. Nocivelli, L. *et al.* established a complete model of the interaction by spray and wall to study the coupling of droplet evaporation heat flux and gas-solid interface boundary conditions, and pointed out the important influencing factors [4]. Lee, C. *et al.* established a steady-state kinetic model of vanadium-based catalyst urea SCR, and optimized it using experimental data, and proposed the optimal conditions for urea SCR in NH_3/NO_x ratio and temperature [5]. Nagaraj, N.S. *et al.* used CFD code, Fire v8.3 to study urea spray, theoretically studied the evaporation of individual urea droplets, and used Lagrangian method to track droplet trajectories, and they simulated in different exhaust gas temperatures and injection position, at last the accuracy of the model was verified by experiments [6]. Li Xiaomin *et al.* studied the distribution of flue gas fluid in the SCR system by establishing a mathematical model, and analyzed the flow field distribution with or without deflector [7]. A large number of studies on urea injection and spray have shown that the urea spray characteristics have an important impact on the overall performance of the SCR, but there are relatively few studies on the gas-liquid two-phase flow inside the spray gun.

In this paper, the flow field changes are simulated, and studied the spray characteristics under different gas path pressure. By comparing the simulation results and experimental results, the accuracy of the model is verified, and it could be used as a simulation platform for the performance optimization of the SCR system.

2. Establishment of Physical Model

The main working principle of the gas-assisted urea spray gun is to mix the compressed air and the UWS in the nozzle, and the mixture is sprayed from a uniform plurality of small injection holes. Due to the rapid fluctuation of the high-speed airflow, the liquid film impact is broken into fine droplet particles. The smaller the droplet, the better the urea vaporization pyrolysis and the higher the urea decomposition rate.

2.1. Geometric Model

Figure 1 is a cross-sectional view of a gas-assisted urea spray gun with a liquid path diameter of 5 mm. Compressed air enters the spray gun from the inlet of

the inlet2. The urea enters the spray gun from the inlet1, and finally the compressed air is in the mixing chamber mixes and the last two phases are ejected from the orifice.

2.2. Meshing and Boundary Condition Setting

Since the whole spray gun model has geometric axis symmetry, in order to reduce the number of grids to reduce the calculation time, the middle plane of the geometric model is simulated during the simulation to improve the simulation calculation efficiency, and the selected medium-surface fluid region mesh is shown in **Figure 2**.

When the boundary conditions are set, the boundary condition of the urea inlet inlet1 is set as the mass flow inlet. Inlet2 is the gas inlet and defines the boundary condition as the pressure inlet. Outlet is the fluid outlet, defined as the pressure outlet, with a pressure of 0 MPa.

The simulation uses Euler multiphase flow, multi-interaction, multiphase separation flow model, and the turbulence model is used in both the liquid phase and the gas phase under the Euler phase, and the turbulence model adopts the $k-\epsilon$ model. The atomizing medium in the spray gun is ideal air, and the atomizing

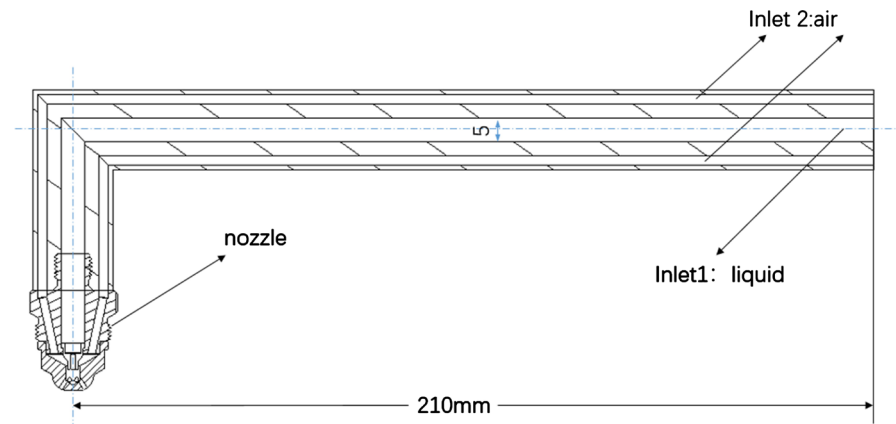


Figure 1. Sectional view of urea spray gun (unit: mm).

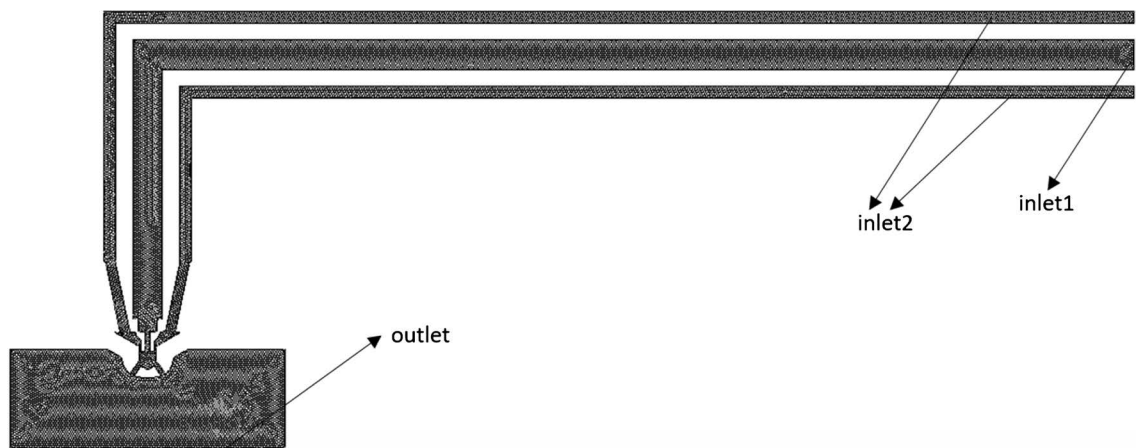


Figure 2. Fluid area meshing diagram.

working medium is UWS with a concentration of 32.5%, and the density thereof is about 1120 kg/m³. Since the physical properties of UWS are very similar to water, the surface tension coefficient and dynamic viscosity of UWS are set to 0.072 N/m and 0.001 Pa·s, respectively, with reference to the fluid properties of the water. For liquid droplet tracking, the S-Gamma model was selected in this paper. In order to meet the actual situation the gravity model was enabled, and then the gas-liquid two-phase flow of the urea nozzle was simulated.

3. The Basic Equation

The flow and interaction of the two-phase flow in the flow field mainly considers the gas-liquid two-phase mixing in the gas cap and the process of ejecting from the nozzle hole. The model follows the three equations of fluid mechanics [8].

Continuity equation:

$$\frac{\partial \rho}{\partial t} + \frac{\partial}{\partial x}(\rho v_x) + \frac{\partial}{\partial y}(\rho v_y) + \frac{\partial}{\partial z}(\rho v_z) = 0 \quad (1)$$

Equation of motion:

$$\frac{\partial v_x}{\partial t} + v_x \frac{\partial v_x}{\partial x} + v_y \frac{\partial v_x}{\partial y} + v_z \frac{\partial v_x}{\partial z} = f_x - \frac{1}{\rho} \frac{\partial p}{\partial x} + \frac{\mu}{\rho} \left(\frac{\partial^2 v_x}{\partial x^2} + \frac{\partial^2 v_x}{\partial y^2} + \frac{\partial^2 v_x}{\partial z^2} \right) \quad (2)$$

$$\frac{\partial v_y}{\partial t} + v_x \frac{\partial v_y}{\partial x} + v_y \frac{\partial v_y}{\partial y} + v_z \frac{\partial v_y}{\partial z} = f_y - \frac{1}{\rho} \frac{\partial p}{\partial y} + \frac{\mu}{\rho} \left(\frac{\partial^2 v_y}{\partial x^2} + \frac{\partial^2 v_y}{\partial y^2} + \frac{\partial^2 v_y}{\partial z^2} \right) \quad (3)$$

$$\frac{\partial v_z}{\partial t} + v_x \frac{\partial v_z}{\partial x} + v_y \frac{\partial v_z}{\partial y} + v_z \frac{\partial v_z}{\partial z} = f_z - \frac{1}{\rho} \frac{\partial p}{\partial z} + \frac{\mu}{\rho} \left(\frac{\partial^2 v_z}{\partial x^2} + \frac{\partial^2 v_z}{\partial y^2} + \frac{\partial^2 v_z}{\partial z^2} \right) \quad (4)$$

Energy equation:

$$v dv = -\frac{1}{\rho} - g dz \quad (5)$$

The traditional turbulence model (k- ϵ equation) can be expressed as:

$$\frac{\partial}{\partial t}(\rho k) + \frac{\partial}{\partial x_i}(\rho k u_i) = \frac{\partial}{\partial x_j} \left[\left(\mu + \frac{\mu_t}{\sigma_k} \frac{\partial k}{\partial x_j} \right) \right] + G_k + G_b + \rho \epsilon - Y_M + S_k \quad (6)$$

In the equation, G_k represents the turbulent flow energy generated by the laminar velocity gradient; G_b is the turbulent flow energy generated by buoyancy; Y_M is the fluctuation due to the transition of the transition in the compressible turbulent flow.

The dynamic behavioral equation of a single cavitation in a liquid, Rayleigh-Plesset, can be expressed as [9]:

$$R_B \frac{d^2 R_B}{dt^2} + \frac{3}{2} \left(\frac{dR_B}{dt} \right)^2 + \frac{2S}{R_B} = \frac{p_v - p}{\rho_1} \quad (7)$$

In the equation, R_B is the bubble radius; S is the liquid phase surface tension coefficient; p_v is the liquid phase saturated vapor pressure; p is the liquid phase confining pressure; ρ_1 is the liquid phase density.

4. Analysis of Simulation Results

By establishing a coupling model of gas-liquid two-phase flow and nozzle outlet flow field in the nozzle, the internal flow and spray characteristics of the nozzle are analyzed to predict whether the spray SMD meets the technical requirements of $\leq 50 \mu\text{m}$. The accuracy of the model is verified by experimental tests, and the model used for optimization of nozzle structure and operating parameters.

4.1. Analysis of Two-Phase Flow Field in Nozzle

Figure 3 shows the distribution of gas-liquid two-phase flow inside the nozzle for different time periods. Before the injection is started, the spray gun is filled with air, and the liquid phase starts to move toward the spray hole. At this time, the gas-liquid interface is curved, the liquid phase and the gas phase collide at the inlet of the mixing chamber, and the liquid phase is torn by the compressed air and spread around. After entering the mixing chamber, the urea is further atomized by the expansion of the compressed air. The liquid phase is mainly concentrated on the centerline axis, and the volume fraction decreases along the radial direction, eventually reaching equilibrium.

The liquid phase passes through the large passage, the reducer, the small passage, the mixing chamber, the spray hole, etc. from the inlet to the outlet. Due to the change of the cross section of the flow passage, the liquid phase is gradually accelerated, and it can be seen that the liquid phase is extremely low before entering the small channel, and the velocity of the small channel is slightly higher. At the bottom of the small channel, liquid phase exchange momentum with the gas phase. At the same time, it is necessary for liquid phase to overcome the local and the resistance loss along the path. Therefore, the pressure is gradually reduced, and the pressure is rapidly reduced at the orifice because the flow rate is rapidly increased, as shown in **Figure 4**.

The simulation calculations were carried out for different injection volumes of 4.5 L/h, 12 L/h and 22.5 L/h for the air pressure of 1 bar and 1.5 bar. It solves the pressure and velocity of the fluid at the exit of the orifice, and then it provides boundary conditions for spray characteristic simulation outside the nozzle. At

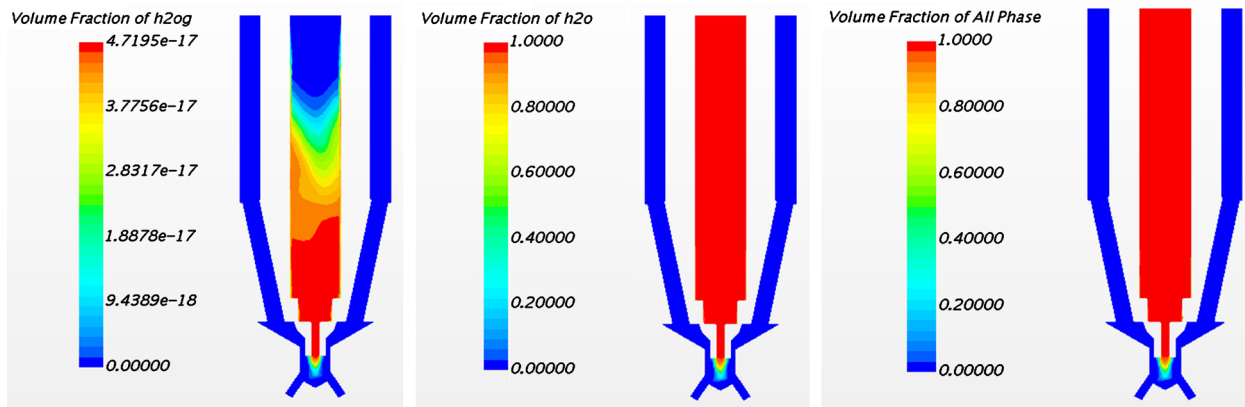


Figure 3. Gas-liquid two-phase distribution in the nozzle.

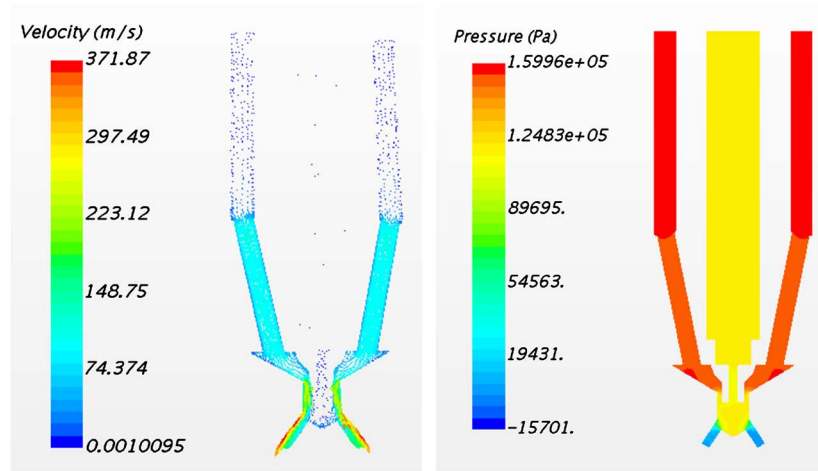


Figure 4. Nozzle internal pressure and velocity distribution.

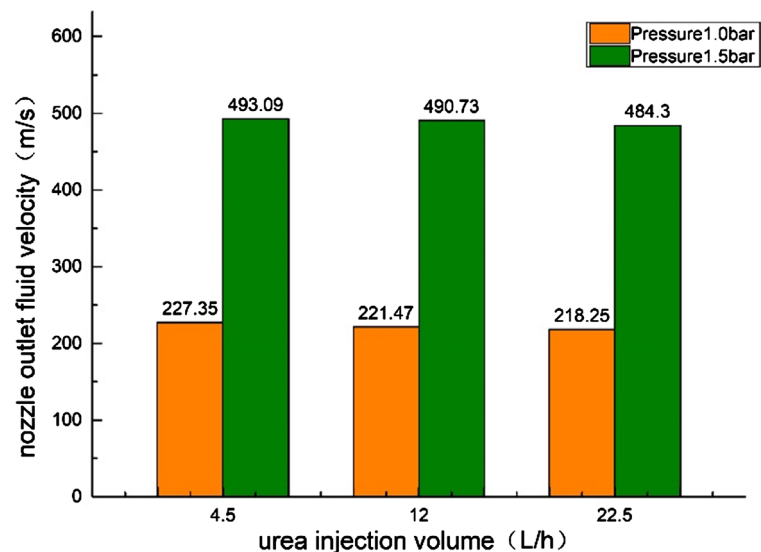


Figure 5. Fluid velocity at different gas path pressures.

this time, the liquid and gas velocities are approximated, and the calculation result is shown in **Figure 5**. It can be seen from the figure that the fluid velocity in 1.5 bar air pressure is 2 times higher than the velocity at 1 bar. And the speed is faster, which promotes the further breaking of the droplet particles. The fluid velocity at the same pressure has a slight decrease with the increase of the injection amount. The reason for the analysis may be that under the same gas pressure, the gas consumption decreases as the liquid flow rate increases, and there is more kinetic energy to break the liquid and accelerate the liquid from the compressed air.

4.2. Analysis of Two-Phase Flow Field outside the Nozzle

The physical parameters such as fluid velocity and nozzle pressure derived from the two-phase flow field in the nozzle are used as the boundary conditions for the spray characteristics simulation. According to the working environment of

the nozzle test, the single spray hole space is selected to simulate the spray particle size. The analysis results are shown in the table as **Table 1**. The results of the average particle diameter values are shown in **Figure 6**.

From the simulation results, it can be seen that the spray particle size distribution spans a large distance. The minimum particle size is 11.22 μm at 1 bar and the maximum particle size is 92.6 μm . The minimum particle size at 1.5 bar is 9.35 μm and the maximum particle size is 80.39 μm . As the axial distance increases, the droplet diameter gradually increases. The maximum and minimum particle sizes of 1.5 bar are both below 1 bar pressure. The reason is that the gas pressure is high, the fluid flows out quickly from the orifice, and the atomization is better. The average particle size at the same pressure has a slight decrease with the increase of flow rate, which may be due to the constant air pressure during the simulation. The increase of the liquid flow rate, the decrease of the gas flow rate, and then there are lack of sufficient gas kinetic energy to break the liquid.

Table 1. Comparison of spray particle sizes for different injection volumes at different pressures.

Injection volume	1 bar particle size simulation analysis	1.5 bar particle size simulation analysis
4.5 L/h		
12 L/h		
22.5 L/h		

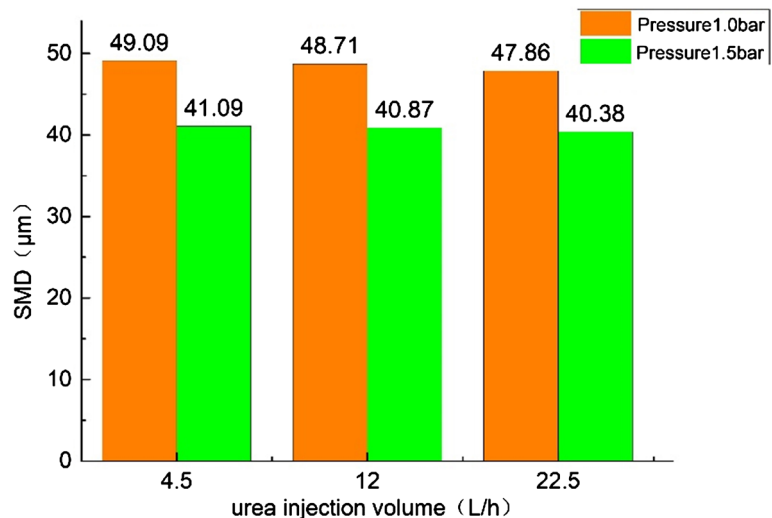


Figure 6. Sauter average particle size under different gas path pressures.

4.3. Spray Cone Angle Simulation

Urea crystallization is a very high probability of failure in SCR systems [10] [11] [12]. The spray cone angle has an important influence on the crystallization of the wall. The excessive spray cone angle may cause the urea to collide with the wall. The spray cone angle is too small, which may result in uneven distribution of NH_3 and reduce the conversion efficiency of SCR. The spray cone angles simulated by the experimental model in this paper are shown in **Table 2**. It can be seen from **Table 2** that the spray cone angle is substantially constant at different gas pressures and different injection amounts.

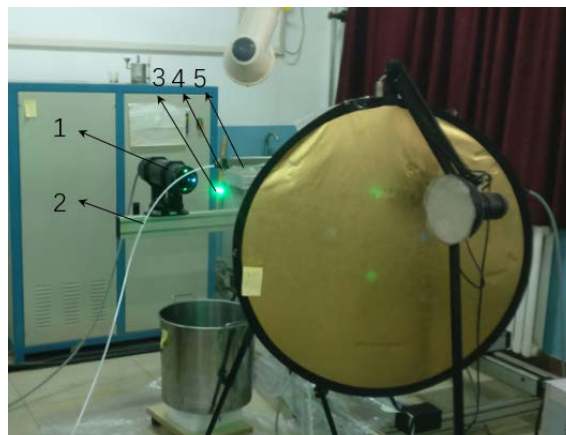
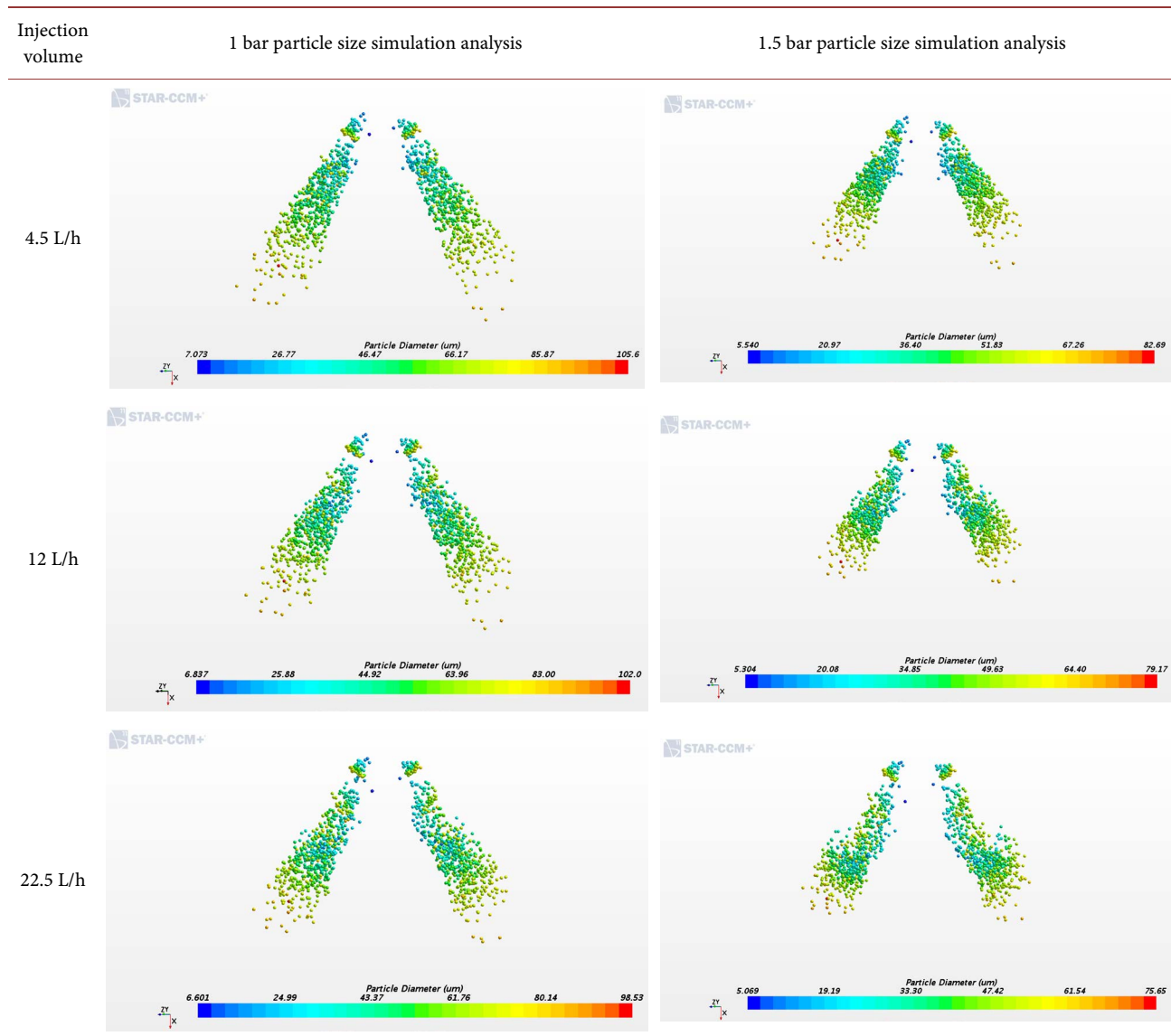
By processing the droplet distribution in the spray field, and taking the outer contour of the droplet group as the boundary condition of the spray, the nozzle cone angle can be obtained, and the spray cone angle can be approximated as 70° , which is sandwiched by the nozzle axis. The angles are consistent, indicating that the amount of injection and the pressure of the gas path have less influence on the cone angle.

5. Test Verification

The spray particle size test uses a three-dimensional particle dynamic analyzer. The instrument measurement range is $0.5 \mu\text{m} - 3000 \mu\text{m}$. The test method is shown in **Figure 7**. The light path emitters can move accurately, and then the spray particle size and droplet speed at different positions can be collected by changing the position of the 3 test points.

The laser particle size tester was used to measure the spray particle size of different urea flows from different positions of the orifice at 1.0 bar and 1.5 bar pressure. The measurement results are shown in **Figure 8**. Tests have shown that the spray particle size is basically equivalent at each flow rate, and the SMD is about $42 - 49 \mu\text{m}$, which is equivalent to the calculation result. It can be seen that the large flow spray particle size is smaller than the small flow particle size

Table 2. Comparison of spray cone angles for different injection volumes at different pressures.



1. Light emitter; 2. Nozzle inlet pipe; 3. Test point; 4. Nozzle; 5. Nozzle intake pipe

Figure 7. Spray particle size test.

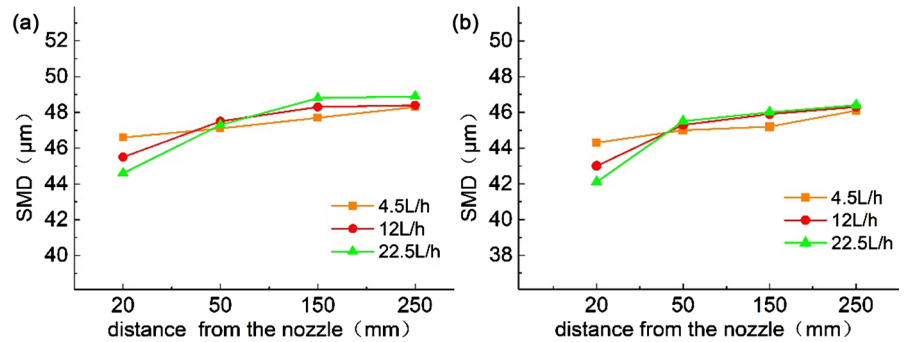


Figure 8. Spray particle size at different flow distances from different orifices. (a) 1.0 bar-SMD; (b) 1.5 bar-SMD.

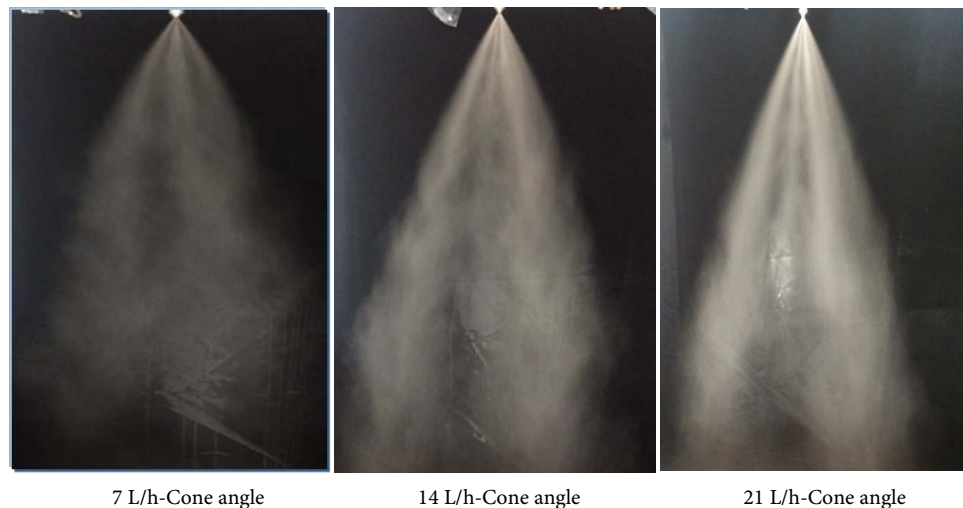


Figure 9. Spray cone angle at different flow rates.

at 20 mm from the nozzle. However, as the jetting distance increases, the large flow particle size exceeds the small flow particle size, which is presumed to be due to spray collision polymerization.

Shooting different flow sprays, roughly measuring the spray cone angle, the results show that the spray cone angles are similar, both about 70° . And the calculation results are basically the same, as shown in **Figure 9**.

6. Conclusions

1) The simulation model established in this paper can accurately simulate the gas-liquid mixing process in the urea spray gun, and can output the velocity of the fluid and the volume fraction of the two phases, providing boundary conditions for the flow field calculation outside the orifice.

2) The simulation found that the spray particle size is mainly related to the gas path pressure, and the larger the gas path pressure, the smaller the SMD. The gas-assisted SCR spray has a small particle size. The lowest and highest average particle diameters at 1.0 bar are $47.86 \mu\text{m}$ and $49.09 \mu\text{m}$. The lowest and highest average particle sizes at 1.5 bar are $40.38 \mu\text{m}$ and $41.09 \mu\text{m}$, and the overall size is less than $50 \mu\text{m}$. The initial particle size distribution span is large, and as the axi-

al distance increases, the droplets become uniform and the spray cone angle does not change with the pressure and urea flow.

3) The calculation results were verified by a three-dimensional particle dynamic analyzer. It was found that the spray particle size was 44 - 49 μm at a pressure of 1.0 bar and the spray particle size was 42 - 47 μm at a pressure of 1.5 bar. The error between the actual droplet SMD and the simulated droplet size does not exceed 5 μm . The actual spray cone angle is maintained at around 70°, which is consistent with the model simulation results. It is necessary to further confirm the spray cone angle simulation and experimental verification of nozzles of different structures. In this paper, the two-phase flow model of the urea spray gun can accurately simulate the urea atomization process in practical applications. It can be used in practical engineering to provide a simulation platform for the overall design of SCR.

Conflicts of Interest

The authors declare no conflicts of interest regarding the publication of this paper.

References

- [1] Johnson, T.V. (2011) Diesel Emissions in Review. SAE Paper, 2011-01-0304.
- [2] Ma, Y. and Wang, J.A. (2016) Control Method for Consistent Performance of Automotive Selective Catalytic Reduction Systems under Variant Aging Conditions. *American Control Conference*, Boston, 6-8 July 2016, 4187-4192.
- [3] Zhao, Y., Lun, H., *et al.* (2011) Experimental Study on Spray Characteristics of Urea Solution in Diesel Engine SCR System. *China National Internal Combustion Engine Society Burning Energy Saving and Purifying Branch 2011 Academic Annual Meeting*, Tianjin, 2011, 8.
- [4] Nocivelli, L., Montenegro, G., Liao, Y., *et al.* (2015) Modeling of Aqueous Urea Solution Injection with Characterization of Spray-Wall Cooling Effect and Risk of Onset of Wall Wetting. *Energy Procedia*, **82**, 38-44.
<https://doi.org/10.1016/j.egypro.2015.11.880>
- [5] Lee, C. (2016) Modeling Urea-Selective Catalyst Reduction with Vanadium Catalyst Based on NH₃ Temperature Programming Desorption Experiment. *Fuel*, **173**, 155-163.
<https://doi.org/10.1016/j.fuel.2016.01.065>
- [6] Nagaraj, N.S., Kapilan, N. and Sadashiva, P.S. (2012) Modeling of Urea-Water Solution Injection Spray in SCR System. *Applied Mechanics & Materials*, **232**, 583-587.
<https://doi.org/10.4028/www.scientific.net/AMM.232.583>
- [7] Li, X. and Wang, L. (2017) Application and Analysis of Baffled Test in Simulation of SCR System. *Ecotechnology*, **23**, 5-9.
- [8] Anderson, J.D. (2007) Computational Fluid Dynamics. Mechanical Industry Press, Berlin.
- [9] Zhao, D., Wang, Q. and Du, M. (2016) Fluent—Based Numerical Simulation of the Cavitation Behavior in the Angle Nozzle. *Journal of Northeastern University (Natural Science)*, **37**, 1283-1287.
- [10] Liu, G., Bao, W., Zhang, W., *et al.* (2018) An Intelligent Control of NH₃ Injection for Optimizing the NO_x/NH₃ Ratio in SCR System. *Journal of the Energy Institute*.

<https://doi.org/10.1016/j.joei.2018.10.008>

- [11] Shang, D., Li, B.K. and Liu, Z.Q. (2019) Large Eddy Simulation of Transient Turbulent Flow and Mixing Process in an SCR Denitration System. *Chemical Engineering Research and Design*, **141**, 279-289. <https://doi.org/10.1016/j.cherd.2018.11.006>
- [12] Kaushal, N., Amsini, S. and Johannes, J. (2018) Numerical Investigation of AdBlue Droplet Evaporation and Thermal Decomposition in the Context of NOX-SCR Using a Multi-Component Evaporation Model. *Energy*, **11**, 222-245. <https://doi.org/10.3390/en11010222>